The EMBO Journal (2008) 27, 406–420 | © 2008 European Molecular Biology Organization | Some Rights Reserved 0261-4189/08
www.embojournal.org

THE EMBO JOURNAL

EMBO open

Dynamic histone H3 methylation during gene induction: HYPB/Setd2 mediates all H3K36 trimethylation

John W Edmunds, Louis C Mahadevan* and Alison L Clayton

Nuclear Signalling Laboratory, Department of Biochemistry, Oxford University, Oxford, UK

Understanding the function of histone modifications across inducible genes in mammalian cells requires quantitative, comparative analysis of their fate during gene activation and identification of enzymes responsible. We produced high-resolution comparative maps of the distribution and dynamics of H3K4me3, H3K36me3, H3K79me2 and H3K9ac across c-*fos* and c-*jun* upon gene induction in murine fibroblasts. In unstimulated cells, continuous turnover of H3K9 acetylation occurs on all K4-trimethylated histone H3 tails; distribution of both modifications coincides across promoter and 5′ part of the coding region. In contrast, K36- and K79-methylated H3 tails, which are not dynamically acetylated, are restricted to the coding regions of these genes. Upon stimulation, transcription-dependent increases in H3K4 and H3K36 trimethylation are seen across coding regions, peaking at 5′ and 3′ ends, respectively. Addressing molecular mechanisms involved, we find that Huntingtin-interacting protein HYPB/Setd2 is responsible for virtually all global and transcription-dependent H3K36 trimethylation, but not H3K36-mono- or dimethylation, in these cells. These studies reveal four distinct layers of histone modification across inducible mammalian genes and show that HYPB/Setd2 is responsible for H3K36 trimethylation throughout the mouse nucleus.

The EMBO Journal (2008) **27,** 406–420. doi:10.1038/sj.emboj.7601967; Published online 20 December 2007
Subject Categories: chromatin & transcription
Keywords: chromatin; histone methyltransferases; histone modifications; HYPB/Setd2; transcription elongation

Introduction

Histone modifications, which include acetylation, phosphorylation, methylation and ubiquitination, play key roles in gene regulation (reviewed in Shilatifard, 2006; Berger, 2007; Bernstein *et al*, 2007; Kouzarides, 2007; Li *et al*, 2007). They are studied by chromatin immunoprecipitation (ChIP) to define their location, by genetic and biochemical analyses to identify enzymes involved and by identification of binding proteins or domains to determine their molecular function. ChIP is widely used to map histone modifications across genes and chromosomes, but their quantification and interpretation is contentious (reviewed in Clayton *et al*, 2006). In particular, high-resolution quantitative comparative studies in synchronised mammalian cells tracking changes in histone modification during transcriptional activation are currently unavailable.

The immediate-early (IE) genes c-*fos* and c-*jun* are rapidly induced in mammalian cells via ERK or p38 MAP kinase cascades. These kinases activate the downstream kinase MSK1/2, which phosphorylates histone H3 and HMGN1 (reviewed in Clayton and Mahadevan, 2003). Phosphorylated histone H3 is subject to continuous dynamic acetylation, creating phosphoacetylated H3 (Barratt *et al*, 1994), which is seen at c-*fos* and c-*jun* upon gene induction (Cheung *et al*, 2000; Clayton *et al*, 2000). Although they are colocalised at these genes, these two modifications are independently regulated by distinct mechanisms (Thomson *et al*, 2001). More recently, we reported that all K4-trimethylated H3 in these cells is also subject to extremely dynamic, continuous turnover of acetylation (Hazzalin and Mahadevan, 2005). ChIP with phosphoacetylated (S10phK9ac) or K4me3-specific antibodies and re-ChIP experiments showed that all three modifications can occur on the same nucleosomes (Hazzalin and Mahadevan, 2005). Because K4me3 was continuously detectable, whereas K9ac and S10ph were transient, we favoured a model whereby K4me3 was the key pre-existing modification, which attracts both dynamic acetylation and stimulus-dependent S10 phosphorylation (reviewed in Clayton *et al*, 2006). Such complex models can only be confirmed by detailed quantitative comparative mapping of these modifications across genes. H3 methylated at lysines 4, 36 or 79 is generally associated with active/permissive chromatin, whereas lysine 9 or 27 methylation is associated with repression (reviewed in Shilatifard, 2006). Within genes, K4me3, K9ac and K14ac occur around start sites of active genes (Liang *et al*, 2004; Bernstein *et al*, 2005; Pokholok *et al*, 2005; Barski *et al*, 2007; Guenther *et al*, 2007; Mikkelsen *et al*, 2007). K4me2 has been reported at start sites of active genes in metazoans (Liang *et al*, 2004; Schneider *et al*, 2004), but is spread throughout coding regions in yeast (Pokholok *et al*, 2005). In contrast, K4me1 is reported towards the 3′ end of active genes (Kouskouti and Talianidis, 2005; Pokholok *et al*, 2005), as have both K36me2 and me3 (Bannister *et al*, 2005;

*Corresponding author. Nuclear Signalling Laboratory, Department of Biochemistry, University of Oxford, South Parks Road, Oxford OX1 3QU, UK. Tel.: +44 01865 285 345; Fax: +44 01865 279 252;
E-mail: louiscm@bioch.ox.ac.uk

Received: 3 September 2007; accepted: 3 December 2007; published online: 20 December 2007

Farris *et al*, 2005; Morillon *et al*, 2005; Pokholok *et al*, 2005; Vakoc *et al*, 2006; Barski *et al*, 2007; Guenther *et al*, 2007; Mikkelsen *et al*, 2007). An exception to this is a transient post-initiation peak of K36me2 and me3 at the yeast *MET16* promoter (Morillon *et al*, 2005). In *Drosophila*, K79me2 occurs throughout coding regions of active genes (Schübeler *et al*, 2004). Likewise, in yeast, K79me3 was found in coding regions, but there was no correlation with gene activity (Pokholok *et al*, 2005). At active mammalian genes, K79me2 and me3 are reported to peak towards the 5′ end of the coding region (Kouskouti and Talianidis, 2005; Vakoc *et al*, 2006), although another study found K79me2 at both promoter and coding regions of active genes (Im *et al*, 2003).

Complications to all such studies include quantitation and comparability of ChIP recovery using different antibodies and the possibility of microheterogeneity at any position, whereby distinct histone modifications, deriving from different cells within a population, are detectable at the same position along a gene. An obvious source of microheterogeneity is the transient dynamic nature of some histone modifications, for example, H3 acetylation described above. A second relates to the fact that some histone-modifying enzymes travel with elongating RNA polymerase II (Pol II), producing elongation-dependent variation across coding regions. In yeast, the K4 methyltransferase SET1/COMPASS complex (Briggs *et al*, 2001; Krogan *et al*, 2002) coimmunoprecipitates with Pol II phosphorylated at Ser 5 in its CTD (Ng *et al*, 2003), a form associated with early elongating complexes (Komarnitsky *et al*, 2000). In contrast, Set2, the yeast K36 methyltransferase (Strahl *et al*, 2002), associates with Pol II phosphorylated at Ser 2 in its CTD (Li *et al*, 2002; Krogan *et al*, 2003; Schaft *et al*, 2003; Xiao *et al*, 2003; Kizer *et al*, 2005), a form of Pol II found increasingly towards the 3′ end of transcribed genes (Komarnitsky *et al*, 2000). K36me then recruits a histone deacetylase (HDAC) complex via interaction with the chromodomain of Eaf3 (Carrozza *et al*, 2005; Joshi and Struhl, 2005; Keogh *et al*, 2005), which is required for suppression of internal transcript initiation in the *STE11* and *FLO8* genes (Carrozza *et al*, 2005). In higher eukaryotic cells, the location of K36me at 3′ coding regions of active genes (Bannister *et al*, 2005; Carrozza *et al*, 2005), the observation that it is dependent upon the CTD kinase p-TEFb (Zhou *et al*, 2004; Eissenberg *et al*, 2007) and sensitive to the transcriptional inhibitor DRB (Vakoc *et al*, 2006) all suggest an elongation-dependent mechanism similar to that in yeast. Potential enzymes include nuclear receptor-binding SET domain-containing protein 1 (NSD1), Smyd2 and the Huntingtin-interacting protein HYPB/SETD2, all of which methylate K36 *in vitro* (Rayasam *et al*, 2003; Sun *et al*, 2005; Brown *et al*, 2006), but questions of which enzyme is relevant *in vivo* and whether it catalyses mono-, di- and/or trimethylation in intact cells are unanswered.

Here, we have comprehensively mapped the distribution of histone H3 K9ac, K4me3, K36me3 and K79me2 across c-*fos* and c-*jun* at high resolution, and demonstrate rapid elongation-dependent changes in K4me3 and K36me3 within the coding regions upon gene activation. These studies reveal four distinct layers of histone modification that may be distinguished across these genes. Using siRNA to knock down the relevant enzymes, we show here that Setd2, the mouse homologue of human Huntingtin-interacting protein HYPB, is responsible for virtually all detectable K36me3, but not K36me2 or K36me1, throughout the nucleus. Consistent with its proposed interaction with RNA Pol II, this enzyme mediates EGF-induced transcription-dependent increase of H3K36 trimethylation at the 3′ ends of c-*fos* and c-*jun*. This represents the first unequivocal demonstration in mammalian cells that a single histone methyltransferase (HMTase) enzyme may be entirely responsible for the totality of a specific state of methylation, that is, trimethylation but not mono- or dimethylation, throughout the nucleus.

Results

We first carried out a comprehensive mapping study to determine the distribution of histone modifications across c-*fos* and c-*jun* in control, EGF-stimulated (Figure 1) or anisomycin-stimulated (Supplementary Figure S1) mouse fibroblasts. A modified ChIP protocol, using MNase instead of sonication to generate predominantly mononucleosomal chromatin (MacDonald *et al*, 2005) was used to produce high-resolution quantitative comparative maps of the distribution and dynamics of H3K4 trimethylation (K4me3), K36 trimethylation (K36me3), K79 dimethylation (K79me2) and K9 acetylation (K9ac) across these genes (Figure 1 and Supplementary Figure S1). Each antibody was first titrated in ChIP to arrive at concentrations that recovered virtually all available epitopes, leaving little or none in the unbound fraction as monitored by western blotting. Peaks of distribution of each modification across these genes are shown graphically (Figure 1B and Supplementary Figure S1B) and as bar charts with error bars (Figure 1C and Supplementary Figure S1C). This yielded highly reproducible maps with striking differences in the amounts of each modification recovered. Their interpretation is extremely complex because of the continuous dynamic turnover of acetylation at these genes, the fact that methylation may occur transiently with the traverse of RNA pol II, and the phenomenon of microheterogeneity of histone modifications at any single position. Evaluating these maps in overview, common trends applying to both c-*fos* and c-*jun* emerge. First, K9ac (Figure 1B, panel i) and K4me3 (panel ii) have remarkably similar overlapping distributions across the start site of both genes. For both modifications, there is a striking dip precisely at the start site of both genes, and the positions of peaks of modification largely coincide. The stability of this colocalisation at all points analysed is consistent with sequential ChIP assays showing these modifications coexist on the same nucleosomes at these positions (Hazzalin and Mahadevan, 2005). The sharp dip in K4me3 and K9ac at the start site on both genes appears to be due to this position lacking a nucleosome and being more accessible, as indicated by MNase sensitivity maps across these genes (Figure 2 and Supplementary Figure S2). These show that the start sites of c-*fos* and c-*jun* are considerably more sensitive to MNase digestion with $<5\%$ (c-*fos* -79, c-*jun* -57) and $<10\%$ (c-*jun* -396) of the corresponding genomic DNA signal remaining after digestion (Figure 2 and Supplementary Figure S2).

In contrast, K36me3 and K79me2 are found exclusively within the coding regions of c-*fos* and c-*jun* (Figure 1B, panels iii and iv). Although they do overlap, their precise distributions appear distinct. K36me3 peaks towards the 3′ end of the

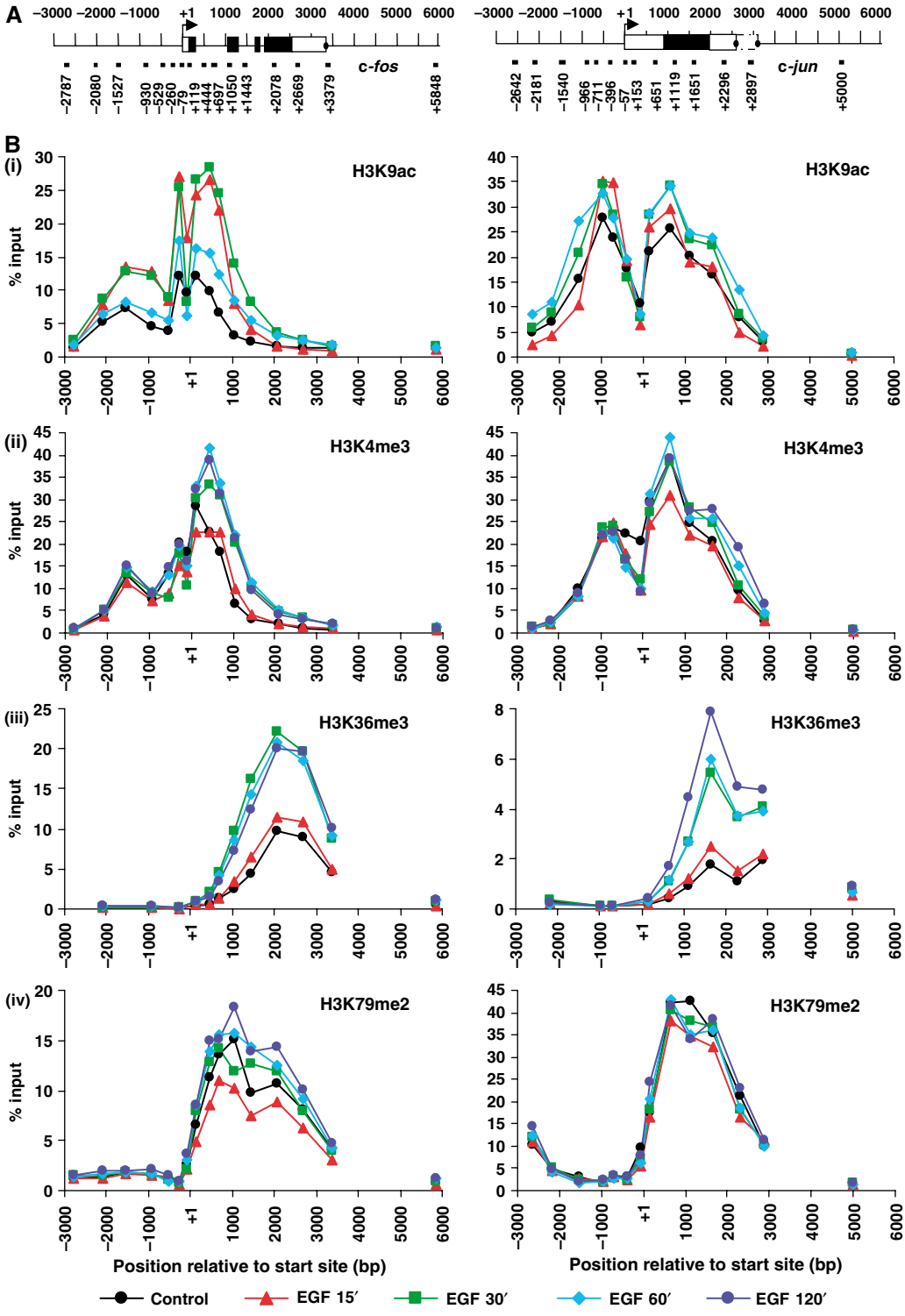

Figure 1 EGF-stimulated distribution of acetylated and methylated histone H3 across c-*fos* and c-*jun*. (**A**) Schematic representation of c-*fos* and c-*jun* showing positions analysed by real-time PCR. Primer positions indicate the 5′ position of the forward primer relative to the transcription start site. Exons are represented by boxes, unfilled for untranslated regions and filled for translated regions. Termination sites are shown as filled circles. (**B**) Quiescent cells were unstimulated (control) or stimulated with EGF (50 ng/ml) for 15, 30, 60 or 120 min and formaldehyde crosslinked mononucleosomes were prepared for ChIP. Aliquots of chromatin were immunoprecipitated with H3K9ac- (i), H3K4me3- (ii), H3K36me3- (iii) or H3K79me2- (iv) specific antibodies. Recovered DNA sequences were quantified by real-time PCR. Average % input recoveries from two independent experiments are plotted. (**C**) Data shown for c-*fos* and c-*jun* are the same as in (B) but plotted in bar chart format with error bars representing the standard deviation (s.d.) of the mean of the two independent experiments. For each ChIP, primers spanning two regions of the inactive β-globin (*hbb*) and the constitutively expressed *gapdh* genes were also analysed (right-hand side graphs) for comparison.

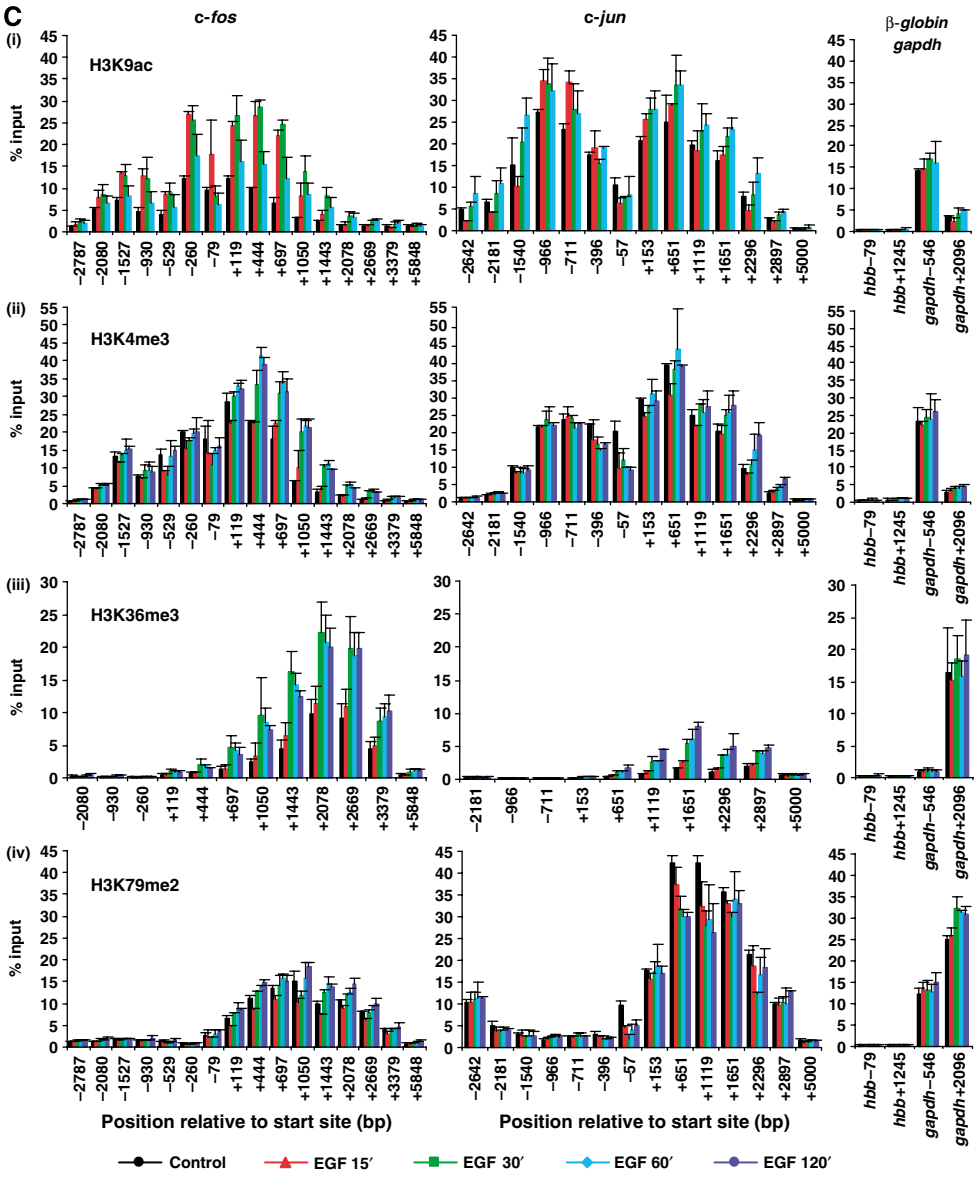

Figure 1 Continued.

coding regions but drops off before the gene's terminus (Figure 1B, panel iii), whereas K79me2 peaks over the 5′ end of the coding region before declining towards the 3′ end (Figure 1B, panel iv). The presence of both these modifications in unstimulated control cells may be attributed either to their being deposited here in previous rounds of transcription prior to quiescence, or to their being part of a transcription-independent pattern of pre-existing, possibly epigenetic, mechanism; there is no evidence either way at present.

Finally, as a negative control, we monitored all four modifications at a site beyond the end of each gene (Figure 1B; c-*fos* +5848; c-*jun* +5000) and found none of these modifications were present there. Stimulation with EGF leads to rapid increases in H3K9ac on c-*fos* across promoter and coding region, peaking at 15 min over the promoter and 30 min over the coding region (Figure 1B, panel i left-side graph). These increases are transient and decrease substantially by 60 min (Figure 1B, panel i), correlating well with kinetics of c-*fos* transcription (Thomson *et al*, 1999). For c-*jun*, basal level of K9ac is much higher than for c-*fos*, and smaller increases are seen upon EGF stimulation, peaking at 60 min (Figure 1B, panel i, right-side graph). The elevated basal level of K9ac on c-*jun* may be due to a low background level of c-*jun* transcription in control cells (Hazzalin and Mahadevan, 2005). K4me3 and K36me3 also increase within the coding regions on c-*fos* and c-*jun* upon stimulation (Figure 1B, panels ii and iii). Compared to K9ac, these increases are slower and more sustained, remaining after 2 h of stimulation (Figure 1B, panels ii and iii). Increases in K4me3 on c-*jun* are much smaller than on c-*fos* (Figure 1B, panel ii).

The entire mapping study was repeated using a different stimulus, anisomycin, which activates these genes predominantly via stress-activated protein kinases (SAPKs) as opposed to the ERK MAP kinase pathway, which EGF utilises (reviewed in Hazzalin and Mahadevan, 2002). This yielded extremely similar MNase sensitivity maps and patterns of distribution and quantitative levels of these modifications

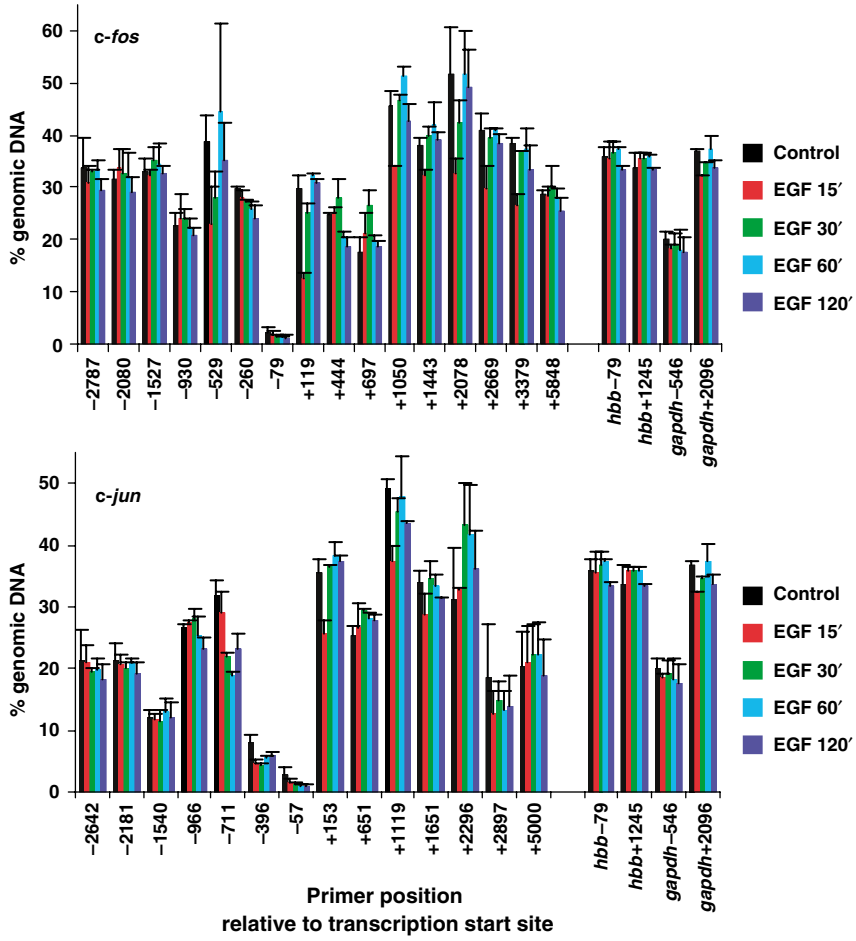

Figure 2 MNase sensitivity across c-*fos* and c-*jun* in quiescent and EGF-stimulated mouse cells. Quiescent cells were unstimulated (control) or stimulated with EGF (50 ng/ml) for 15, 30, 60 or 120 min and formaldehyde crosslinked mononucleosomes were prepared. Equivalent amounts of DNA were isolated from each sample (the DNA is from the same (input) chromatin samples used for the ChIP assays shown in Figure 1 and Supplementary Figure S1) and specific sequences were quantified by real-time PCR. MNase sensitivity is expressed as % of amplifiable DNA sequence in the chromatin sample relative to that in an equivalent amount of intact genomic DNA (more digestion within a region is reflected by fewer intact template molecules that are amplifiable by PCR). Average values from two independent experiments are plotted with s.d. Primers spanning two regions of the *hbb* and *gapdh* genes were also analysed and the data are included on both graphs for comparison (c-*fos* upper panel, c-*jun* lower panel).

across each gene (Supplementary Figures S1 and S2), testifying to the high reproducibility of the methodology used here.

Finally, we address a concern that activation of these genes may produce marked changes of nucleosomes occupancy across the gene, thereby skewing the ChIP recovery data provided at various time points after induction. First, there is no indication of a great change in MNase sensitivity at various time points after stimulation (Figure 2 and Supplementary Figure S2), suggesting that average nucleosomal occupancy at any position did not vary greatly upon gene activation. Second, we carried out ChIP using anti-H3 antibodies directed to the unmodified C terminus across these genes (Supplementary Figure S3A and B, panel i), and this too showed no major changes in recovery upon gene activation, confirming indications from MNase sensitivity maps. As expected, there was good correspondence between the relative H3 occupancy and the MNase sensitivity maps at all points compared across the genes (Supplementary Figure S3A and B, panels ii and iii; see for example, the dip across the start site), indicating that MNase sensitivity seen here is a good approximation of average nucleosomal occupancy.

EGF-induced increases in H3K4me3 and H3K36me3 within c-fos and c-jun coding regions are dependent on transcription elongation

As shown in yeast (reviewed in Gerber and Shilatifard, 2003; Hampsey and Reinberg, 2003; Sims *et al*, 2004), stimulation-dependent increases in K4me3 and K36me3 across coding regions suggest a link with elongating Pol II, a possibility we tested with the transcriptional inhibitor DRB. Quantitative reverse transcription PCR (qRT–PCR) shows that DRB ablates induction of c-*fos* and c-*jun* (Figure 3A). This correlates with loss of Pol II across the coding region of both genes under these conditions, shown by ChIPs using anti-Pol II antibodies raised against its N terminus (Figure 3B). Similar results were obtained at several different positions within the coding regions of c-*fos* and c-*jun* (Supplementary Figure S4A), except for +444 of c-*fos*, which showed increased Pol II loading in response to DRB at later time points. This may be explained by the transcriptional pause site reported at this region (Mechti *et al*, 1991; Coulon *et al*, 1999).

EGF-induced increases in K4me3 and K36me3 within the coding regions of both genes were abolished by DRB pretreatment (Figure 3C, left and middle panels). Other

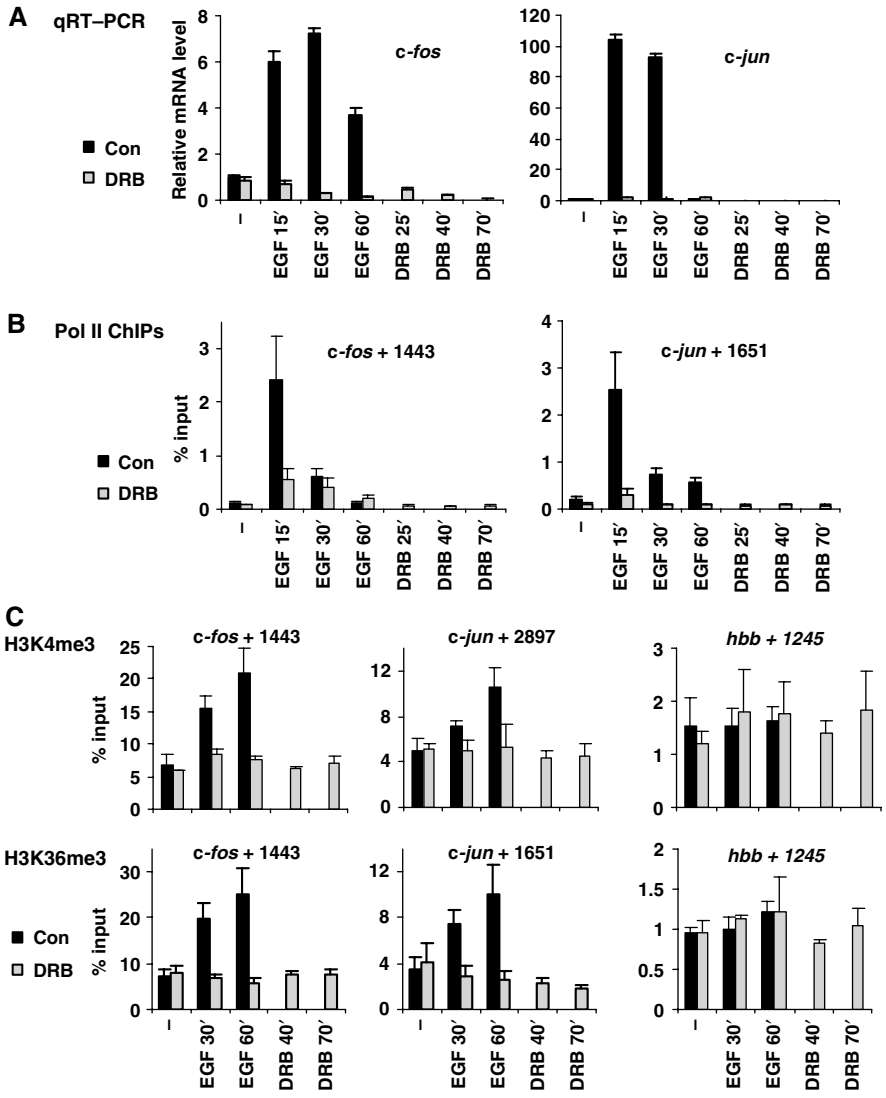

Figure 3 EGF-induced increases in H3K4me3 and H3K36me3 within c-*fos* and c-*jun* are transcription-dependent. (**A**) Quiescent cells were pretreated (10 min) with DRB (25 μg/ml) or untreated (con) prior to stimulation with EGF (50 ng/ml) for 15, 30 or 60 min or no-stimulation (−). Quiescent cells were also treated with DRB alone for 25, 40 or 70 min as controls, respectively. Total mRNA was isolated and relative levels of c-*fos* and c-*jun* mRNA were quantified by qRT–PCR with normalisation to *gapdh* mRNA. A representative experiment is shown. Error bars represent the s.d. from triplicate PCRs. (**B**) Formaldehyde crosslinked mononucleosomes were prepared from quiescent cells treated as in (A) and used for ChIPs with an anti-RNA-polymerase-II (Pol II) antibody. Recovery of c-*fos* and c-*jun* coding DNA sequences were quantified by real-time PCR. Average % input recoveries and s.d. from 3–4 independent experiments are plotted. (**C**) ChIPs and real-time PCR were performed as described in (B) using H3K4me3- (top panel) and H3K36me3- (bottom panel) specific antibodies. Amplicons analysed are indicated above each graph. Average % input recoveries and s.d. from 3–4 independent experiments are plotted.

coding region positions within c-*fos* and c-*jun* gave similar results (Supplementary Figure S4B and C). As expected, in the negative control *hbb* coding region, no significant change in either modification was observed in response to EGF or DRB (Figure 3C, right panel). Thus, EGF-induced increases in K4me3 and K36me3 within coding regions of these genes are dependent on transcription elongation.

Setd2 is non-redundantly responsible for H3K36 trimethylation in mouse fibroblasts

In *Saccharomyces cerevisiae*, *Schizosaccharomyces pombe* and *Neurospora crassa*, Set2 is an H3K36 methyltransferase responsible for mono-, di- and trimethylation (Strahl *et al*, 2002; Adhvaryu *et al*, 2005; Morris *et al*, 2005; Chu *et al*, 2006). In mammals, several candidates have been proposed. The first discovered, NSD1, has *in vitro* HMTase activity towards H3K36 and H4K20 (Rayasam *et al*, 2003). Second, a SET domain protein that interacts with the Huntington's Disease gene (*HD*) product, HYPB/SETD2, also methylates H3K36 *in vitro* and, via its C-terminal Pol II interaction domain, can bind to phosphorylated Pol II (Sun *et al*, 2005). Finally, Smyd2 has HMTase activity towards H3K36 *in vitro*, and interacts with Sin3 HDAC complexes (Brown *et al*, 2006). None of these studies addressed their ability to methylate H3K36 *in vivo*, or the specific states (mono, di or tri) of methylation for which they might be responsible. Dimethyl-H3K36 antibodies were used in the NSD1 and Smyd2 studies, but capacity for mono- or trimethylation was not analysed.

Using NCBI protein BLAST search, we identified mouse homologues of yeast Set2 (data not shown). Setd2 (the mouse homologue of human HYPB/SETD2) and NSD1 (among

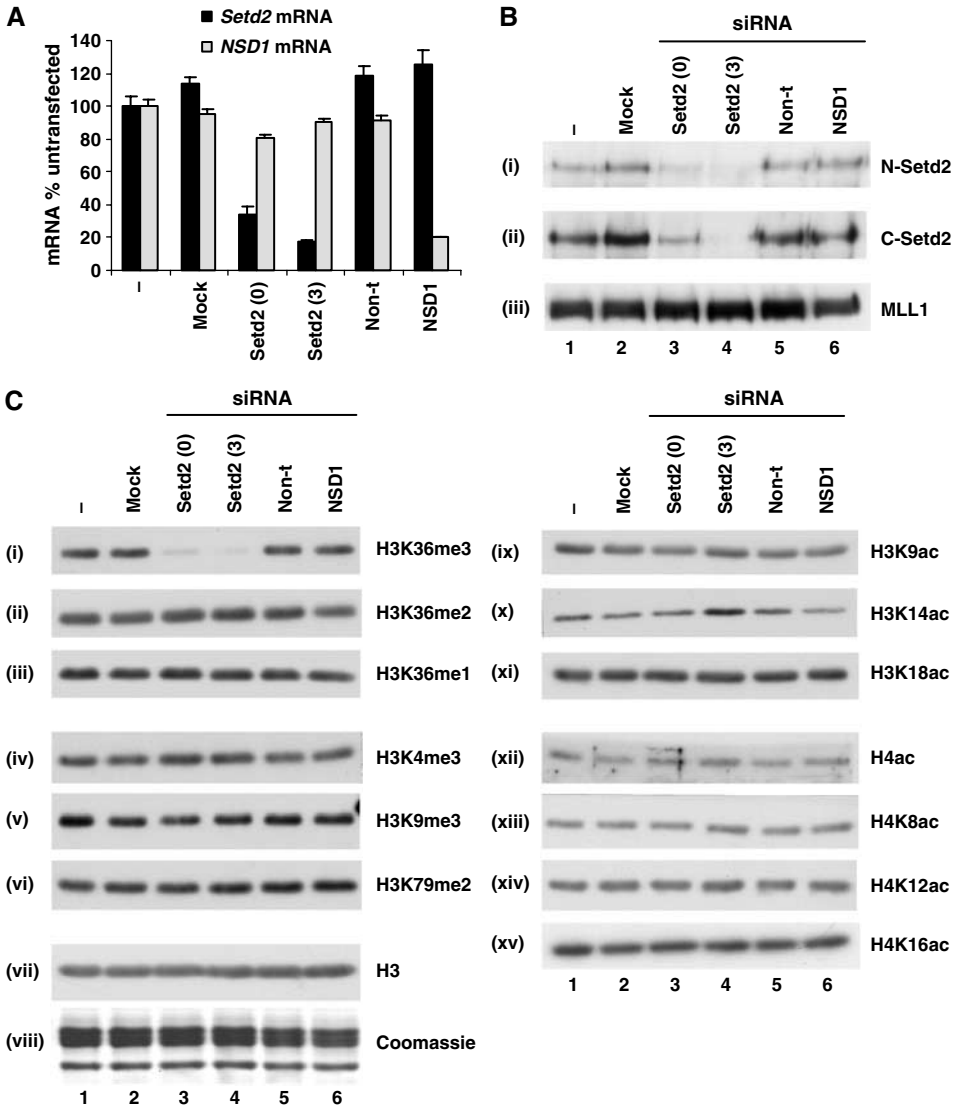

Figure 4 Setd2 is a non-redundant H3K36-specific trimethyltransferase. (**A**) Cells were untransfected (−), mock transfected (no siRNA, mock) or transfected with Setd2 (0 and 3, two different siRNAs), NSD1 or non-targeting (non-t) siRNAs. Total mRNA was isolated 24 h later and relative levels of *Setd2* and *NSD1* mRNA were quantified by qRT–PCR and normalised to *gapdh* mRNA. A representative experiment is shown. Error bars represent the s.d. from triplicate PCRs. (**B**) Cells were transfected as in (A) and crude nuclear lysates were prepared 48 h later. Lysates were separated by 8% SDS–PAGE and transferred to PVDF membrane for immunoblotting with two different Setd2 antibodies (N-Setd2 (i) and C-Setd2 (ii)) and an MLL1 antibody (iii) as a control. (**C**) Crude nuclear lysates were prepared as in (B), separated by 15% SDS–PAGE and either Coomassie-stained (viii) or transferred to PVDF membrane for immunoblotting with various methyl (i–vi) or acetyl (ix–xv) modification-specific histone antibodies, as indicated in the figure. H4ac is an anti-histone H4 pan-acetyl antibody. Unmodified H3 (H3, vii) was used as a loading control.

others) had significant homology. In view of this homology, and the fact that HYPB/SETD2 has a Pol II interaction domain (Sun *et al*, 2005), we investigated Setd2 and NSD1 as possible H3K36 methyltransferases in mouse fibroblasts.

Two different siRNAs targeting *Setd2* transcripts knocked down *Setd2* mRNA levels by >60% (Setd2 0) and >80% (Setd2 3) (Figure 4A). siRNA targeting *NSD1* transcripts knocked down *NSD1* mRNA levels by >80% (Figure 4A). These were specific, as mock-transfected cells, or non-targeting siRNA, did not show similar effects (Figure 4A). Additionally, Setd2- or NSD1-specific siRNAs did not knock down mRNAs of other genes tested (Figure 4A and data not shown). We raised and characterised N- and C-terminal Setd2 antibodies to confirm that Setd2 protein levels were specifically diminished as a result of its mRNA knockdown (Figure 4B, panels i and ii; Supplementary Figure S5). We were not able to assess NSD1 protein levels, as a good antibody is currently unavailable. This became less relevant since the Setd2 knockdown produced a clear H3K36 trimethylation defect.

Total cellular K36me3 was virtually absent in the Setd2 knockdowns (Figure 4C, panel i), whereas K36me2 and me1 levels remain unaffected (Figure 4C, panels ii and iii). In contrast, NSD1 knockdown had no effect on mono-, di- or trimethylation of K36 (Figure 4C, panels i–iii). Additionally, total levels of K4me3, K9me3 or K79me2 were unchanged in either Setd2 or NSD1 knockdowns (Figure 4C, panels iv–vi). Therefore, Setd2 appears to be a non-redundant methyltransferase specific for trimethylation of H3K36. This is the first demonstration in intact cultured cells of a H3K36-specific methyltransferase whose knockdown results in abrogation of virtually all trimethylation, but not mono- or dimethylation.

It is not possible, however, to distinguish from these experiments if HYPB/Setd2 can catalyse all states of modification culminating in K36 trimethylation, or just the final conversion of dimethylated K36 to the trimethylated state. Since there are several recent reports of a link between H3K36 methylation and histone deacetylation in yeast (Carrozza *et al*, 2005; Joshi and Struhl, 2005; Keogh *et al*, 2005), we also analysed global levels of various H3 and H4 acetyl modifications in Setd2 knockdown cells. No significant reproducible changes were observed for any acetyl modification (Figure 4C, panels ix–xv).

Setd2 is responsible for H3K36 trimethylation at IE and housekeeping genes

Next, we used ChIP to analyse all states of K36 methylation at c-*fos*- and c-*jun* coding regions (mid and 3′ end) after Setd2 knockdown. Four housekeeping genes were also analysed; *glyceraldehyde-3-phosphate-dehydrogenase* (*gapdh*), *RNA-polymerase III subunit b* (*polr3b*), *glutaminyl-tRNA synthetase* (*glnrs*) and *cyclophilin b* (*cycb*) (shown schematically in Figure 5A).

Trimethyl K36

Setd2 knockdown produced almost complete loss of total cellular K36me3 in these cells (Figure 5B) and a marked reduction of K36me3 at c-*fos*- and c-*jun* coding regions (Figure 5C, panel i). Stimulation with EGF for 60 min resulted in a 2.7- to 3.4-fold increase in the K36me3 observed at these regions (black bars panel i), whereas in the Setd2 knockdown, induced levels of K36me3 were much smaller—1.3- to 1.8-fold (middle bars panel i). K36me3 was also decreased by $>50\%$ within the coding regions of *gapdh*, *cycb*, *polr3b* and *glnrs* after Setd2 knockdown (Figure 5D, panel i). Setd2 therefore appears to be responsible for both basal and inducible K36me3 at IE gene coding regions, and K36me3 levels at constitutively active genes.

Mono- and dimethyl K36

For all points tested, the recovery of nucleosomes with H3 bearing mono- and dimethyl K36 was very much lower (>10-fold) than that of trimethyl K36 (Figure 5C). In untransfected cells, there is no increase in mono- and dimethylated K36 upon activation of c-*fos* and c-*jun* (Figure 5C, panels ii and iii), indicating no correlation between these modifications and transcription. In Setd2 knockdown cells, there is no decrease in these low levels of K36me2 or me1 within the coding regions of c-*fos* and c-*jun*, with the exception of the c-*jun* $+1651$ region where there is a small decrease in K36me2 (Figure 5C, panel ii). Thus, in general Setd2 does not appear to be responsible for the low levels of mono- or dimethyl K36 at these regions.

As described for c-*fos* and c-*jun*, recovery of K36me1 and me2 was also very much lower than that of K36me3 at coding regions of *gapdh*, *cycb*, *polr3b* and *glnrs* (Figure 5D). In fact, these levels are very similar to that seen at the inactive *hbb* coding region (Figure 5C, panels ii and iii bottom graphs). Knockdown of Setd2 resulted in slightly higher levels of K36me2 and K36me1 at these positions (Figure 5D, panels ii and iii) but recoveries remain relatively very low. Thus, K36me2 and K36me1 levels do not seem to correlate with active transcription as K36me3 does, and Setd2 does not appear to be responsible for these modifications. By their nature, knockdowns do not produce the complete loss of any enzyme and low residual activity of the remaining HYPB/Setd2 enzyme may explain the incomplete loss of H3K36 sometimes seen.

Loss of H3K36me3 does not affect the kinetics of IE gene transcription, intragenic transcription or expression of constitutively active genes

To investigate the potential role of K36me3 in transcriptional regulation, the effect of K36me3 loss on the transcription of IE and constitutively active genes was assessed by qRT–PCR (Figure 6). As shown previously, knock down of Setd2 mRNA (Figure 6A) led to virtually complete loss of all detectable K36me3 (Figure 6D). The gene induction kinetics of c-*fos*, c-*jun* and two other IE genes, *core promoter element binding protein* (*CPBP)* and *MAP kinase phosphatase 1* (*MKP1)*, was examined (Figure 6B). A recent report in yeast has shown that increased K36me leads to delayed induction of the *HIS4* gene, whereas elimination of K36me accelerates *HIS4* induction (Nelson *et al*, 2006). However, loss of K36me3 did not affect the kinetics of induction of any gene tested here (Figure 6B). Second, the steady-state mRNA levels of four constitutively active genes (*cycb*, *polr3b*, *glnrs* and *gapdh*) were assessed in the absence of K36me3, and no significant changes were observed for any transcript (Figure 6C). Furthermore, we did not observe any intragenic transcription from c-*fos*, c-*jun* or *gapdh* in K36me3-depleted cells (Figure 6E). This is in contrast to the observations in yeast where K36me appears to create a less permissive chromatin structure throughout yeast gene coding regions by recruiting HDAC complexes (Rpd3) via interaction with the chromodomain of Eaf3 (Carrozza *et al*, 2005; Joshi and Struhl, 2005; Keogh *et al*, 2005). Loss of K36me leads to increased acetylation, K4me3 and Pol II loading within specific gene coding regions and intragenic transcript initiation from the *FLO8* and *STE11* genes (Carrozza *et al*, 2005; Joshi and Struhl, 2005; Keogh *et al*, 2005; Kizer *et al*, 2005). Similar to the lack of any intragenic transcription in K36me3-depleted mouse fibroblasts (Figure 6E), we do not detect any increased H3 or H4 acetylation at 3′ regions of IE or housekeeping genes (Supplementary Figure S6), nor any change in Pol II occupancy at these genes (Supplementary Figure S7). These studies do not reveal a clear parallel at c-*fos* and c-*jun* in mammalian cells for the relationship between H3K36 methylation and histone deacetylation previously seen in yeast.

Discussion

Four different layers of histone modifications can now be distinguished across inducible genes in mammalian cells. The first, which includes K4me3 across the start site as well as K79me2 and K36me3 in the coding region (Figure 1) are pre-existing, possibly epigenetic histone modifications detectable in quiescent G0 cells. The second relates to dynamic turnover of histone acetylation by the action of HATS and HDACs, which affects all K4me3-modified H3 in the mouse nucleus (Hazzalin and Mahadevan, 2005; reviewed in Clayton *et al*, 2006). Both of these are detectable in quiescent cells. Upon stimulation, a third signalling-dependent set, which includes H3 phosphorylation at IE genes (Chadee *et al*, 1999; Cheung *et al*, 2000; Clayton *et al*, 2000) or H4 acetylation at *hsp70* (Thomson *et al*, 2004) becomes evident, also seen mostly

across the start site. Finally, there are DRB-sensitive modifications restricted to coding regions of these genes that are dependent upon passage of Pol II, such as enhanced K4me3 and K36me3 (Figure 3C). Thus, a combination of epigenetic, dynamic, kinase- and Pol II-dependent histone modifications is required to fully explain their region and stimulus-specific appearance across these genes.

Setd2 mediates H3K36 trimethylation at the 3′ end of active gene coding regions

Enhancement of K36me3 peaks towards the 3′ end of the induced c-*fos* and c-*jun* genes. There is relatively low recovery of K36me2 and me1, and no increase upon stimulation. Further, mono- and dimethyl K36 states do not correlate with transcription as similar low levels (~1% input) are

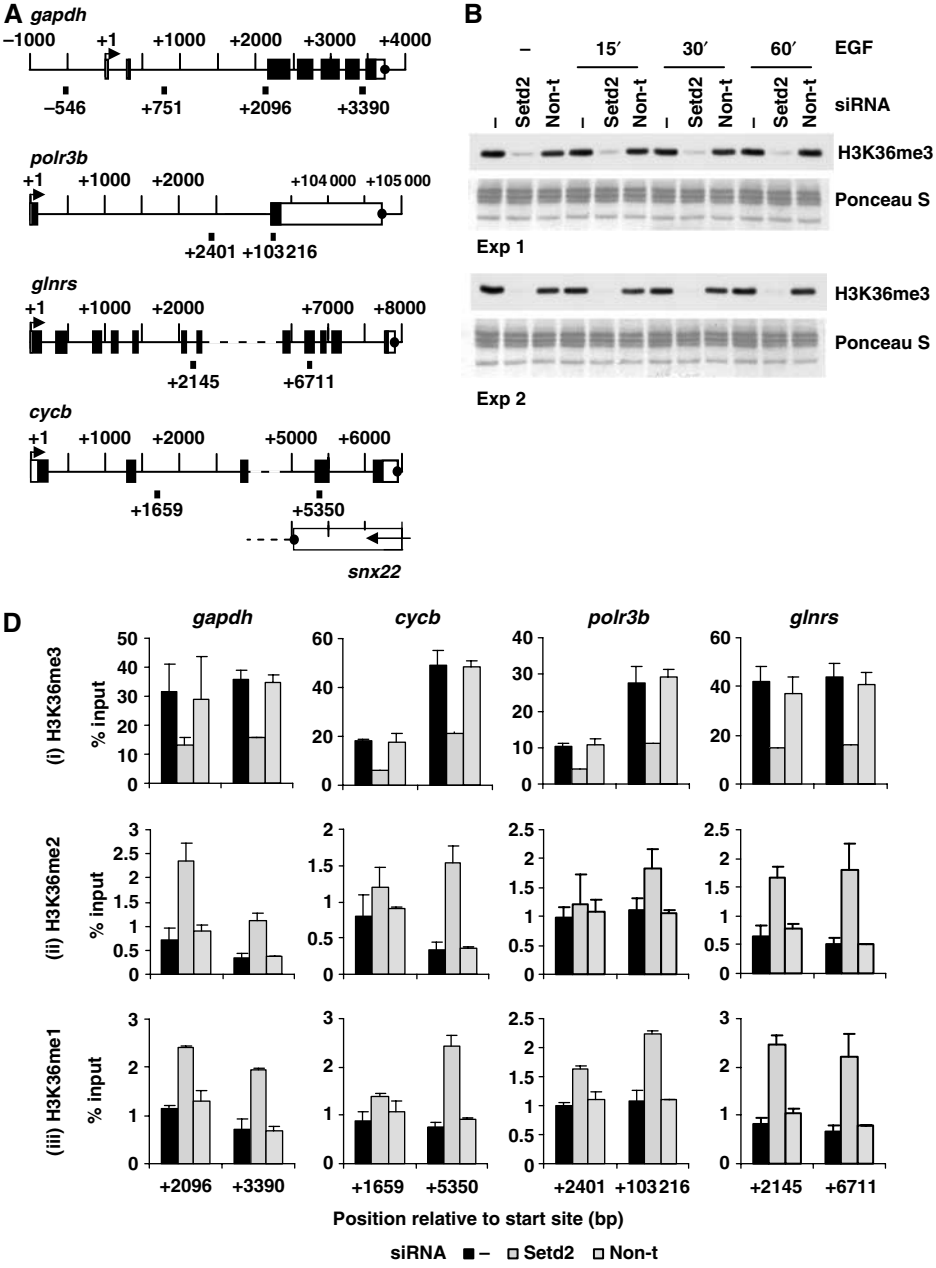

Figure 5 Setd2 is responsible for H3K36 trimethylation at IE and housekeeping genes. (**A**) Schematic representation of the *gapdh*, *polr3b*, *glnrs* and *cycb* housekeeping genes showing regions amplified by primers used for real-time PCR. Primer positions shown indicate 5′ position of the forward primer relative to the transcription start site. Exons are represented by boxes, unfilled for untranslated regions and filled for translated regions. Transcription termination sites are shown as filled circles. (**B**) Cells were untransfected (–) or transfected with Setd2 or non-targeting (non-t) siRNA. Cells were quiesced 24 h later, and after a further 24 h were unstimulated (–) or stimulated with EGF (50 ng/ml) for 15–60 min. Formaldehyde crosslinked mononucleosomes were prepared and aliquots of each sample were heated to reverse the crosslinks, separated by 15% SDS–PAGE, transferred to PVDF and immunoblotted with an H3K36me3-specific antibody. Membranes were stained with Ponceau S before immunoblotting to verify even loading. (**C**) Aliquots of formaldehyde crosslinked mononucleosomes prepared as in (B) were used in ChIP assays with H3K36me3- (i), H3K36me2- (ii) and H3K36me1- (iii) specific antibodies. Recovery of c-*fos*, c-*jun* and *hbb* coding region sequences were quantified by real-time PCR. Average % input recoveries and s.d. from two independent experiments are plotted. Regions analysed are indicated to the left of the panels. (**D**) Aliquots of formaldehyde crosslinked mononucleosomes from unstimulated cells prepared as in (B) were used in ChIP assays with H3K36me3- (i), H3K36me2- (ii) and H3K36me1- (iii) specific antibodies. Recovery of *gapdh*, *cycb*, *polr3b* and *glnrs* coding region sequences were quantified by real-time PCR. Average % input recoveries and s.d. from two independent experiments are plotted.

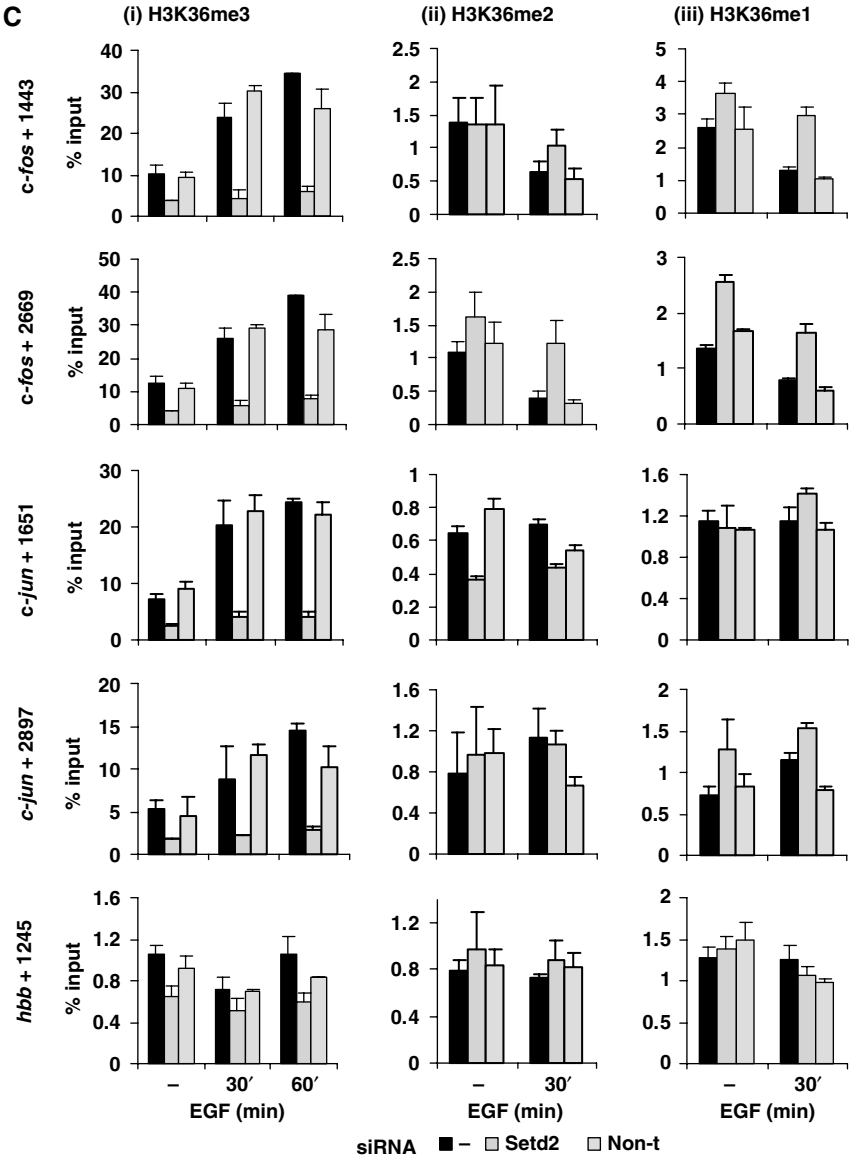

Figure 5 Continued.

detectable at active or inactive genes (Figure 5C *hbb*, and 5D, panels ii and iii). This emphasises the importance of considering quantitative aspects of ChIP when evaluating reports in yeast (Krogan *et al*, 2003; Morillon *et al*, 2005; Rao *et al*, 2005) and metazoa (Zhou *et al*, 2004; Bannister *et al*, 2005; Miao and Natarajan, 2005) showing that both di- and trimethylated K36 are associated with active genes.

The distinctive distribution of K4me3 (peaking 5′) and K36me3 (peaking 3′) across these active genes (Figure 1B and Supplementary Figure S1B, panels ii and iii) may result from selective methyltransferase recruitment to differentially phosphorylated Pol II, as shown in yeast (reviewed in Hampsey and Reinberg, 2003). MLL1, a mammalian H3K4-specific methyltransferase, is recruited to the 5′ end of active genes (Milne *et al*, 2002; Nakamura *et al*, 2002; Dou *et al*, 2005; Guenther *et al*, 2005). MLL1 or components of MLL1-containing complexes interact with Pol II phosphorylated at the Ser 5 position of its CTD (Hughes *et al*, 2004; Milne *et al*, 2005), the form of Pol II associated with 5′ coding regions (Komarnitsky *et al*, 2000). HYPB/SETD2 has been shown to coimmunoprecipitate with Ser 2-phosphorylated Pol II (Sun *et al*, 2005), suggesting that like Set2, it may 'piggyback' with Pol II across the gene to direct co-transcriptional trimethylation of K36 at the 3′ coding regions of c-*fos* and c-*jun*. Attempts to use our N- and C-terminal antibodies to show association of HYPB/Setd2 with these regions by ChIP were unsuccessful (data not shown), but as we do not have a positive control for these experiments, they are not conclusive.

Selectivity and multi-enzyme systems for H3K36 methylation in mammals

In contrast to its homologue Set2, which is responsible for all three methyl states in *S. cerevisiae*, *S. pombe* and *N. crassa* (Adhvaryu *et al*, 2005; Morris *et al*, 2005; Chu *et al*, 2006), Setd2 is specifically responsible for K36 trimethylation in mouse cells (Figures 4C and 5B–D). This suggests a more complex multi-enzyme system for K36 methylation in higher

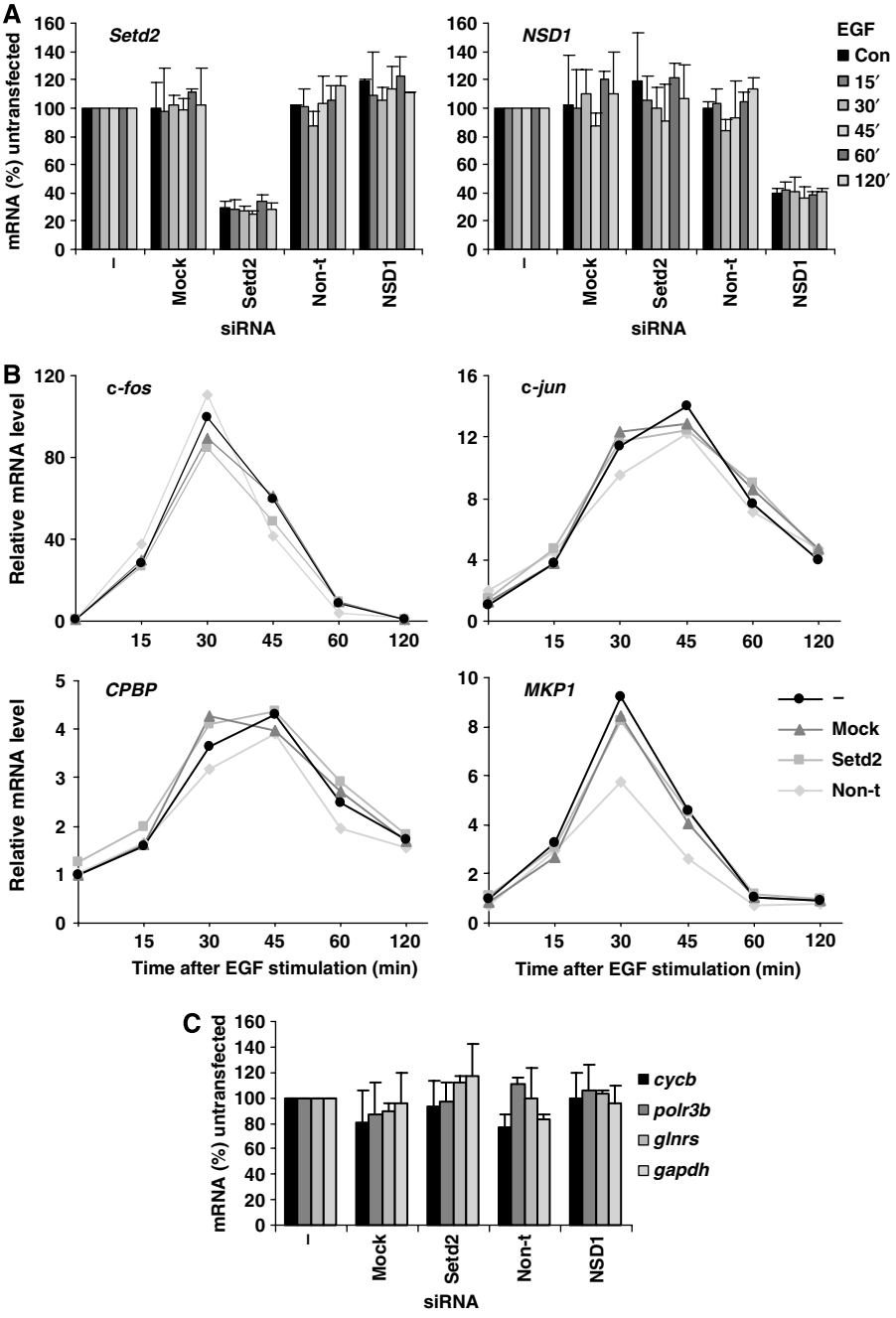

Figure 6 Effects of H3K36me3 knockdown on gene expression levels: lack of intragenic transcription from IE genes or *gapdh*. (**A**) C3H 10T$\frac{1}{2}$ cells were untransfected (−), mock transfected (no siRNA, mock) or transfected with Setd2, non-targeting (non-t) or NSD1 siRNA. Cells were quiesced 24 h later, and after a further 24 h left untreated (con) or treated with EGF (50 ng/ml) for 15–120 min. Total RNA was isolated and relative levels of *Setd2* and *NSD1* mRNA were quantified by qRT–PCR and normalised to 18S rRNA. Average values and s.d. from two independent experiments are plotted. (**B**) Cells were transfected and stimulated and total RNA isolated as in (A). Kinetics of c-*fos*, c-*jun*, *CPBP* and *MKP1* gene expression was assessed by qRT–PCR and normalised to 18S rRNA. Average values and s.d. from two independent experiments are plotted. (**C**) Cells were transfected as in (A), left unstimulated and levels of *cycb*, *polr3b*, *glnrs* and *gapdh* mRNA quantified by qRT–PCR, with normalisation to 18S rRNA. Average values and s.d. from two independent experiments are plotted. (**D**) Cells were transfected and stimulated as in (A) and cellular protein was isolated from the same TRIzol® reagent preparations used for RNA extraction. Protein was separated by 15% SDS–PAGE and transferred to PVDF membrane for immunoblotting with an H3K36me3 (i)-specific antibody. Ponceau S staining of histones was performed to verify even loading (ii). (**E**) C3H 10T$\frac{1}{2}$ cells were untransfected (−) or transfected with Setd2, non-targeting (non-t) or NSD1 siRNA. Cells were quiesced 24 h later, and after a further 24 h left untreated (con) or treated with EGF (50 ng/ml) for 15–60 min. Total mRNA was isolated and northern blotting carried out with 3′ c-*fos* (i) and 3′ c-*jun* (ii) probes and a full-length *gapdh* cDNA probe (iii).

eukaryotes, similar to that for K4 methylation. Set1 is the only enzyme shown to methylate K4 in yeast, whereas many enzymes exist in mammals, including hSet1, MLL1–4, Set7/9, SMYD2 and Meisetz (reviewed in Ruthenburg *et al*, 2007). Some of these are methyl-state specific. For example, Meisetz specifically catalyses trimethylation of K4 *in vivo* (Hayashi *et al*, 2005). Mouse NSD1 was previously shown to dimethylate K36 *in vitro* (Rayasam *et al*, 2003), but the

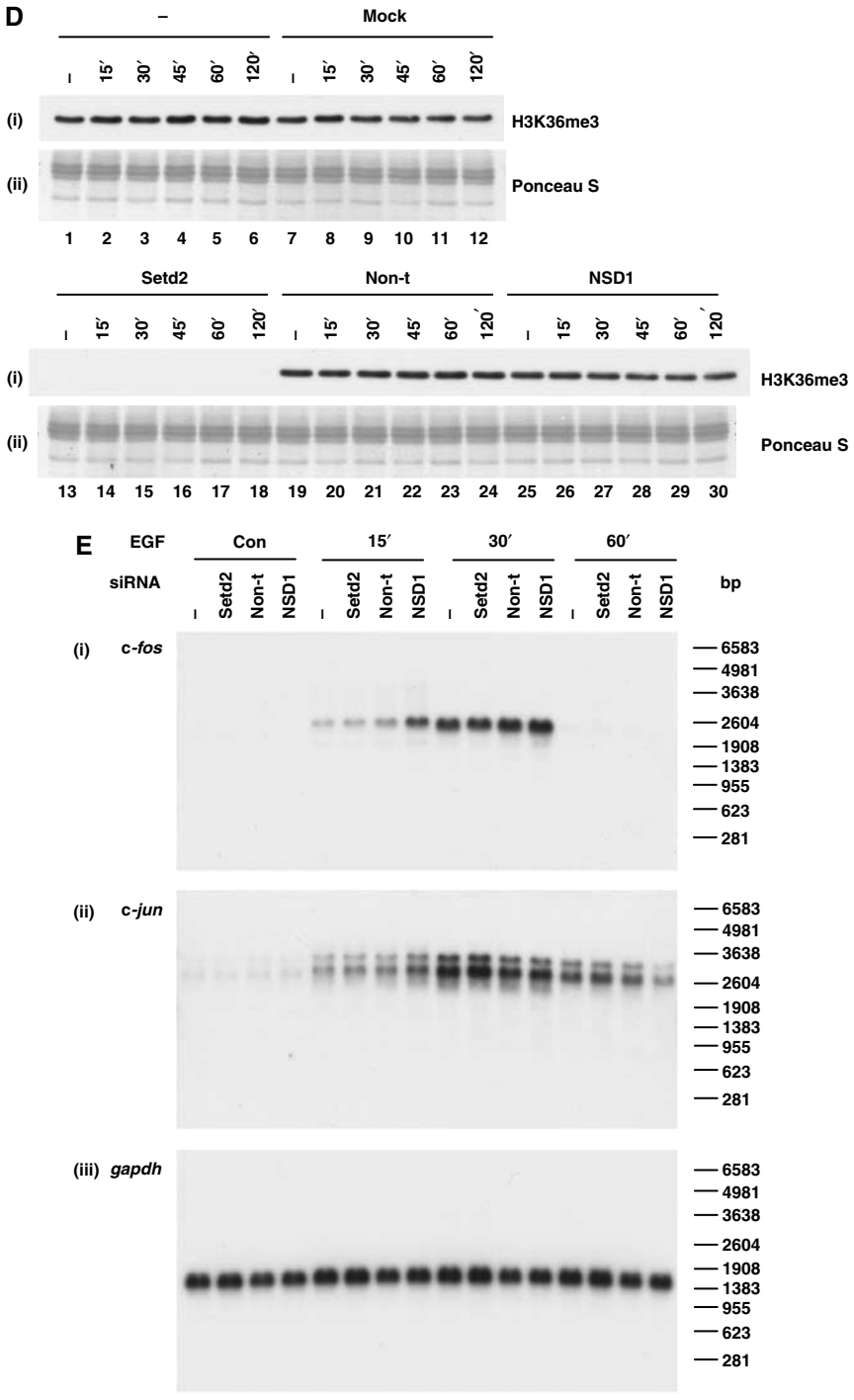

Figure 6 Continued.

mono- and trimethyl states were not analysed. In this study, NSD1 did not appear to be responsible for total nuclear mono-, di- or trimethyl K36 (Figure 4C, panels i–iii) nor that at c-*fos* and c-*jun* (data not shown). Other potential K36 mono- and/or dimethyltransferases include the closely related NSD2 and NSD3 proteins, or the Smyd2 protein recently found to dimethylate K36 *in vitro* (Brown *et al*, 2006). This study indicates an unexpectedly strict relationship between a specific state of H3K36 methylation and a single methyltransferase enzyme, a finding that may eventually be found relevant for other HMTases in mammals.

Materials and methods

Materials

Anisomycin, TSA and DRB were supplied by Sigma and rhEGF by Promega. siRNAs were synthesised by Dharmacon. PCR primers and 5′ FAM 3′ TAMRA probes were synthesised by Eurogentec.

Antibodies and peptides

H3K36me3 (ab9050), H3K36me1 (ab9048), H3K18ac (ab1191) and unmodified H3 (ab7834 for western and ab1791 for ChIP assays) antibodies were from Abcam. H3K36me2 (07-369), H3K9me3 (07-442), H3K14ac (07-353), H3K79me2 (07-366), H4K8ac (06-760), H4K12ac (06-761) and H4K16ac (06-762) antibodies were

from Upstate, and Pol II antibody (sc-899) was from Santa Cruz. Anti-pan-acetyl H4 was a gift from Dr Tim Hebbes (University of Portsmouth). C-terminal MLL1 antibody was a gift from Dr James Hsieh (Washington University, St Louis).

In-house antibodies were raised by PTU/BS (Pentlands Science Park, Penicuik, Midlothian, UK), using peptides from Alta Bioscience (University of Birmingham). Rabbit anti-H3K9ac and anti-H3K4me3 antisera were raised against the peptides ARTKQTARK(ac)STGGKAPRKQLC and ARTK(me3)QTARKSGGC, respectively. N-Setd2 and C-Setd2 antisera were raised in rabbit and sheep, against the peptides MERRGKYTSKLERESKRTSEC and RGTKR PDDRYDTPTSKKKVRC, corresponding to amino acids 1–20 and 1560–1579 of mouse Setd2 (NCBI accession no.: XP_900231), respectively. All peptides were synthesised with C-terminal cysteine for coupling to keyhole limpet haemocyanin (KLH).

Cell culture

C3H 10T1/2 mouse fibroblasts were cultured in DMEM containing 10% (v/v) fetal calf serum (FCS) and 2 mM glutamine. Cells (70–90% confluent) were quiesced by transferring to DMEM with 0.5% (v/v) FCS and 2 mM glutamine for 24–28 h prior to stimulation and treatment as described.

Acid extraction of histones and western blotting

Extraction of histones, SDS–PAGE and western blotting were carried out essentially as described previously (Cano *et al*, 1995; Clayton *et al*, 2000). Setd2 and histones were resolved on 8 and 15% polyacrylamide gels, respectively. Antibodies were used at the following dilutions: H3K4me3 and H3K9ac, 1:10,000; H3K36me3, H3K36me2 and H3K79me2, 1:5000; H4K8ac, H4K12ac and H4K16ac, 1:4000; H3K14ac, MLL1, C-Setd2 and N-Setd2, 1:2500; H3K36me1, H3K18ac and unmodified H3, 1:2000; H3K9me3 and pan-acetyl H4, 1:1000.

Transfection with siRNA

Cells were cultured to 40–60% confluence before washing with, and transferring to OptiMEM® I medium (Invitrogen). Cells were transfected with siRNA (50 nM in final medium) using Lipofectamine 2000 (Invitrogen) according to the manufacturer's instructions. After 5 h, an equal volume of DMEM medium containing 20% (v/v) FCS and 2 mM glutamine was added. Total RNA was extracted 24 or 48 h after transfection as described below. For protein analysis, cells were harvested in lysis buffer (0.2% (v/v) Triton X-100, 10 mM HEPES pH 8, 0.25 M sucrose, 1.5 mM $MgCl_2$, 10 mM NaCl, 10 mM sodium butyrate, 20 mM β-glycerophosphate, 100 μM sodium orthovanadate, 1 μM microcystin and protease inhibitors (Mahadevan and Bell, 1990)) 48 h after transfection. Crude nuclei were pelleted by centrifugation and resuspended in SDS–PAGE sample buffer. Cells were quiesced 24 h after transfection as described above. Crosslinked mononucleosomes were prepared 48 h after transfection as detailed below.

RNA extraction, qRT–PCR and northern blotting

Total RNA was extracted using TRIzol® reagent (Invitrogen) according to the manufacturer's instructions. For qRT–PCR, contaminating DNA was removed using the TURBO DNA-free™ kit (Ambion), and 0.5 μg of RNA was reverse-transcribed using the SuperScript™ III First-Strand Synthesis kit (Invitrogen). cDNA was then quantified by real-time PCR. For northern analysis, 5 μg of RNA was resolved on formaldehyde/agarose gels, transferred to nylon membrane (Hybond-N+, Amersham) and hybridised with probes as detailed in Hazzalin *et al* (1997). c-*fos* (+2091 −3109) and c-*jun* (+1853 −2920) 3′ gene fragments for probes were amplified by PCR from cDNA, labelled by random priming (Amersham RediPrime II kit) and sequentially hybridised to membranes.

Preparation of crosslinked mononucleosomes and ChIP

Formaldehyde crosslinked mononucleosomes were prepared as described in Macdonald *et al* (2005). Antibodies (10 μl H3K36me3/Pol II or 5 μl H3K36me2/H3K36me1/H3K79me2/H3K4me3 serum/H3K9ac serum/Pan-acetyl H4 serum) were added to chromatin aliquots (~25–30 μg DNA) and rotated for 2 h at 4°C. Protein A-sepharose beads (~5 mg) pre-blocked with 10 μg sonicated herring sperm DNA and BSA (0.02% final concentration after addition to chromatin) were then added and samples rotated for a further 2 h at 4°C. Beads were recovered by centrifugation, and unbound supernatant chromatin was retained. Beads were washed sequentially with 3× RIPA buffer (Clayton *et al*, 2000) without phosphatase or protease inhibitors, 3× RIPA containing 500 mM NaCl and 2× TE (10 mM Tris–HCl pH 7.5, 1 mM EDTA). Input and antibody-bound chromatins were incubated at 65°C overnight to reverse crosslinks. Samples were treated with RNase A (100 μg/ml, 1 h, 37°C) followed by proteinase K (100 μg/ml, 3 h, 37°C) before phenol/chloroform extraction of DNA. Extracted DNA was ethanol precipitated and redissolved in 10 mM Tris–HCl pH 8.0, 0.1 mM EDTA. The presence of specific gene sequences was then quantified by real-time PCR.

Real-time PCR

Real-time PCR was performed using the ABI Prism 7000 sequence detection system (Applied Biosystems). All primers were designed with Primer Express 2.0 software (Applied Biosystems). All c-*fos*, c-*jun*, *gapdh* and *hbb* amplicons were detected by the 5′ nuclease (Taqman) assay using 5′ FAM 3′ TAMRA-labelled probes and qPCR Mastermix Plus (Eurogentec). All other amplicons were detected by the SYBR® Green assay using SYBR® Green PCR Master Mix (Applied Biosystems). Sequences of primers and probes and detailed conditions are available on request. PCR reactions were carried out in triplicate or duplicate.

For ChIP assays, standard curves (serially diluted sonicated genomic DNA) were included in every plate to ensure bound and input sample dilutions were within the linear range. Data were analysed by the C_T method and plotted as % input recovered in the bound fraction for each amplicon, calculated by the following formula: % input recovery = [100/(input fold dilution/bound fold dilution)] × $2^{(\text{input } C_T - \text{bound } C_T)}$, where no fold dilution = 1. For qRT–PCR, data were analysed by relative quantification using the standard curve method (see Applied Biosystems user bulletin 2). All raw data from micrococcal nuclease sensitivity and ChIP experiments are available upon request.

Note added in proof

During review of this manuscript, Bell *et al* (2007) reported that in Drosophila, dHypb is responsible for the trimethylated state of H3K36, in agreement with our findings in mammalian cells. However, the global increase in H4K16 acetylation reported upon dHypb knockdown in Drosophila is not seen in mammalian cells used here (Figure 4C).

Supplementary data

Supplementary data are available at *The EMBO Journal* Online (http://www.embojournal.org).

Acknowledgements

We thank Drs Fiona Myers and Alan Thorne (University of Portsmouth) for advice on real-time PCR in the early stages of this work, and Dr James Hsieh (Washington University, St Louis) for the MLL1 antibody. We thank all members of the Nuclear Signalling Laboratory for help and discussions throughout the course of this work. JWE is supported by an MRC:CASE award with Syngenta. This work was funded by a Wellcome Trust Programme Grant (065373/Z/01/Z).

References

Adhvaryu KK, Morris SA, Strahl BD, Selker EU (2005) Methylation of histone H3 lysine 36 is required for normal development in *Neurospora crassa*. *Eukaryot Cell* **4:** 1455–1464

Bannister AJ, Schneider R, Myers FA, Thorne AW, Crane-Robinson C, Kouzarides T (2005) Spatial distribution of di- and tri-methyl lysine 36 of histone H3 at active genes. *J Biol Chem* **280:** 17732–17736

Barratt MJ, Hazzalin CA, Cano E, Mahadevan LC (1994) Mitogen-stimulated phosphorylation of histone H3 is targeted to a small hyperacetylation-sensitive fraction. *Proc Natl Acad Sci USA* **91:** 4781–4785

Barski A, Cuddapah S, Cui K, Roh TY, Schones DE, Wang Z, Wei G, Chepelev I, Zhao K (2007) High-resolution profiling of histone methylations in the human genome. *Cell* **129:** 823–837

Bell O, Wirbelauer C, Hild M, Scharf AN, Schwaiger M, Macalpine DM, Zilbermann F, van Leeuwen F, Bell SP, Imhof A, Garza D, Peters AH, Schübeler D (2007) Localized H3K36 methylation states define histone H4K16 acetylation during transcriptional elongation in *Drosophila*. *EMBO J* (advance online publication, 15 November 2007, doi:10.1038/sj.emboj.7601926)

Berger SL (2007) The complex language of chromatin regulation during transcription. *Nature* **447:** 407–412

Bernstein BE, Kamal M, Lindblad-Toh K, Bekiranov S, Bailey DK, Huebert DJ, McMahon S, Karlsson EK, Kulbokas III EJ, Gingeras TR, Schreiber SL, Lander ES (2005) Genomic maps and comparative analysis of histone modifications in human and mouse. *Cell* **120:** 169–181

Bernstein BE, Meissner A, Lander ES (2007) The mammalian epigenome. *Cell* **128:** 669–681

Briggs SD, Bryk M, Strahl BD, Cheung WL, Davie JK, Dent SY, Winston F, Allis CD (2001) Histone H3 lysine 4 methylation is mediated by Set1 and required for cell growth and rDNA silencing in *Saccharomyces cerevisiae*. *Genes Dev* **15:** 3286–3295

Brown MA, Sims III RJ, Gottlieb PD, Tucker PW (2006) Identification and characterization of Smyd2: a split SET/MYND domain-containing histone H3 lysine 36-specific methyltransferase that interacts with the Sin3 histone deacetylase complex. *Mol Cancer* **5:** 26

Cano E, Hazzalin CA, Kardalinou E, Buckle RS, Mahadevan LC (1995) Neither ERK nor JNK/SAPK MAP kinase subtypes are essential for histone H3/HMG-14 phosphorylation or c-fos and c-jun induction. *J Cell Sci* **108:** 3599–3609

Carrozza MJ, Li B, Florens L, Suganuma T, Swanson SK, Lee KK, Shia WJ, Anderson S, Yates J, Washburn MP, Workman JL (2005) Histone H3 methylation by Set2 directs deacetylation of coding regions by Rpd3S to suppress spurious intragenic transcription. *Cell* **123:** 581–592

Chadee DN, Hendzel MJ, Tylipski CP, Allis CD, Bazett-Jones DP, Wright JA, Davie JR (1999) Increased Ser-10 phosphorylation of histone H3 in mitogen-stimulated and oncogene-transformed mouse fibroblasts. *J Biol Chem* **274:** 24914–24920

Cheung P, Tanner KG, Cheung WL, Sassone-Corsi P, Denu JM, Allis CD (2000) Synergistic coupling of histone H3 phosphorylation and acetylation in response to epidermal growth factor stimulation. *Mol Cell* **5:** 905–915

Chu Y, Sutton A, Sternglanz R, Prelich G (2006) The BUR1 cyclin-dependent protein kinase is required for the normal pattern of histone methylation by SET2. *Mol Cell Biol* **26:** 3029–3038

Clayton AL, Hazzalin CA, Mahadevan LC (2006) Enhanced histone acetylation and transcription: a dynamic perspective. *Mol Cell* **23:** 289–296

Clayton AL, Mahadevan LC (2003) MAP kinase-mediated phosphoacetylation of histone H3 and inducible gene regulation. *FEBS Lett* **546:** 51–58

Clayton AL, Rose S, Barratt MJ, Mahadevan LC (2000) Phosphoacetylation of histone H3 on c-fos- and c-jun-associated nucleosomes upon gene activation. *EMBO J* **19:** 3714–3726

Coulon V, Veyrune JL, Tourkine N, Vie A, Hipskind RA, Blanchard JM (1999) A novel calcium signaling pathway targets the c-fos intragenic transcriptional pausing site. *J Biol Chem* **274:** 30439–30446

Dou Y, Milne TA, Tackett AJ, Smith ER, Fukuda A, Wysocka J, Allis CD, Chait BT, Hess JL, Roeder RG (2005) Physical association and coordinate function of the H3 K4 methyltransferase MLL1 and the H4 K16 acetyltransferase MOF. *Cell* **121:** 873–885

Eissenberg JC, Shilatifard A, Dorokhov N, Michener DE (2007) Cdk9 is an essential kinase in *Drosophila* that is required for heat shock gene expression, histone methylation and elongation factor recruitment. *Mol Genet Genomics* **277:** 101–114

Farris SD, Rubio ED, Moon JJ, Gombert WM, Nelson BH, Krumm A (2005) Transcription-induced chromatin remodeling at the c-myc gene involves the local exchange of histone H2A. *Z J Biol Chem* **280:** 25298–25303

Gerber M, Shilatifard A (2003) Transcriptional elongation by RNA polymerase II and histone methylation. *J Biol Chem* **278:** 26303–26306

Guenther MG, Jenner RG, Chevalier B, Nakamura T, Croce CM, Canaani E, Young RA (2005) Global and Hox-specific roles for the MLL1 methyltransferase. *Proc Natl Acad Sci USA* **102:** 8603–8608

Guenther MG, Levine SS, Boyer LA, Jaenisch R, Young RA (2007) A chromatin landmark and transcription initiation at most promoters in human cells. *Cell* **130:** 77–88

Hampsey M, Reinberg D (2003) Tails of intrigue: phosphorylation of RNA polymerase II mediates histone methylation. *Cell* **113:** 429–432

Hayashi K, Yoshida K, Matsui Y (2005) A histone H3 methyltransferase controls epigenetic events required for meiotic prophase. *Nature* **438:** 374–378

Hazzalin CA, Cuenda A, Cano E, Cohen P, Mahadevan LC (1997) Effects of the inhibition of p38/RK MAP kinase on induction of five fos and jun genes by diverse stimuli. *Oncogene* **15:** 2321–2331

Hazzalin CA, Mahadevan LC (2002) MAPK-regulated transcription: a continuously variable gene switch? *Nat Rev Mol Cell Biol* **3:** 30–40

Hazzalin CA, Mahadevan LC (2005) Dynamic acetylation of all lysine 4-methylated histone H3 in the mouse nucleus: analysis at c-fos and c-jun. *PLoS Biol* **3:** e393 (doi:10.1371/journal.pbio.0030393)

Hughes CM, Rozenblatt-Rosen O, Milne TA, Copeland TD, Levine SS, Lee JC, Hayes DN, Shanmugam KS, Bhattacharjee A, Biondi CA, Kay GF, Hayward NK, Hess JL, Meyerson M (2004) Menin associates with a trithorax family histone methyltransferase complex and with the hoxc8 locus. *Mol Cell* **13:** 587–597

Im H, Park C, Feng Q, Johnson KD, Kiekhaefer CM, Choi K, Zhang Y, Bresnick EH (2003) Dynamic regulation of histone H3 methylated at lysine 79 within a tissue-specific chromatin domain. *J Biol Chem* **278:** 18346–18352

Joshi AA, Struhl K (2005) Eaf3 chromodomain interaction with methylated H3-K36 links histone deacetylation to Pol II elongation. *Mol Cell* **20:** 971–978

Keogh MC, Kurdistani SK, Morris SA, Ahn SH, Podolny V, Collins SR, Schuldiner M, Chin K, Punna T, Thompson NJ, Boone C, Emili A, Weissman JS, Hughes TR, Strahl BD, Grunstein M, Greenblatt JF, Buratowski S, Krogan NJ (2005) Cotranscriptional set2 methylation of histone H3 lysine 36 recruits a repressive Rpd3 complex. *Cell* **123:** 593–605

Kizer KO, Phatnani HP, Shibata Y, Hall H, Greenleaf AL, Strahl BD (2005) A novel domain in Set2 mediates RNA polymerase II interaction and couples histone H3 K36 methylation with transcript elongation. *Mol Cell Biol* **25:** 3305–3316

Komarnitsky P, Cho EJ, Buratowski S (2000) Different phosphorylated forms of RNA polymerase II and associated mRNA processing factors during transcription. *Genes Dev* **14:** 2452–2460

Kouskouti A, Talianidis I (2005) Histone modifications defining active genes persist after transcriptional and mitotic inactivation. *EMBO J* **24:** 347–357

Kouzarides T (2007) Chromatin modifications and their function. *Cell* **128:** 693–705

Krogan NJ, Dover J, Khorrami S, Greenblatt JF, Schneider J, Johnston M, Shilatifard A (2002) COMPASS, a histone H3 (lysine 4) methyltransferase required for telomeric silencing of gene expression. *J Biol Chem* **277:** 10753–10755

Krogan NJ, Kim M, Tong A, Golshani A, Cagney G, Canadien V, Richards DP, Beattie BK, Emili A, Boone C, Shilatifard A, Buratowski S, Greenblatt J (2003) Methylation of histone H3 by Set2 in *Saccharomyces cerevisiae* is linked to transcriptional elongation by RNA polymerase II. *Mol Cell Biol* **23:** 4207–4218

Li B, Carey M, Workman JL (2007) The role of chromatin during transcription. *Cell* **128:** 707–719

Li J, Moazed D, Gygi SP (2002) Association of the histone methyltransferase Set2 with RNA polymerase II plays a role in transcription elongation. *J Biol Chem* **277:** 49383–49388

Liang G, Lin JC, Wei V, Yoo C, Cheng JC, Nguyen CT, Weisenberger DJ, Egger G, Takai D, Gonzales FA, Jones PA (2004) Distinct localization of histone H3 acetylation and H3-K4 methylation to the transcription start sites in the human genome. *Proc Natl Acad Sci USA* **101:** 7357–7362

Macdonald N, Welburn JP, Noble ME, Nguyen A, Yaffe MB, Clynes D, Moggs JG, Orphanides G, Thomson S, Edmunds JW, Clayton AL, Endicott JA, Mahadevan LC (2005) Molecular basis for the recognition of phosphorylated and phosphoacetylated histone H3 by 14-3-3. *Mol Cell* **20:** 199–211

Mahadevan LC, Bell JC (1990) Phosphate-labelling studies of receptor tyrosine kinases. In *Receptors: a Practical Approach*, Hulme EC (ed), pp 181–201. Oxford: IRL press

Mechti N, Piechaczyk M, Blanchard JM, Jeanteur P, Lebleu B (1991) Sequence requirements for premature transcription arrest within the first intron of the mouse c-fos gene. *Mol Cell Biol* **11:** 2832–2841

Miao F, Natarajan R (2005) Mapping global histone methylation patterns in the coding regions of human genes. *Mol Cell Biol* **25:** 4650–4661

Mikkelsen TS, Ku M, Jaffe DB, Issac B, Lieberman E, Giannoukos G, Alvarez P, Brockman W, Kim TK, Koche RP, Lee W, Mendenhall E, O'Donovan A, Presser A, Russ C, Xie X, Meissner A, Wernig M, Jaenisch R, Nusbaum C *et al* (2007) Genome-wide maps of chromatin state in pluripotent and lineage-committed cells. *Nature* **448:** 553–560

Milne TA, Briggs SD, Brock HW, Martin ME, Gibbs D, Allis CD, Hess JL (2002) MLL targets SET domain methyltransferase activity to Hox gene promoters. *Mol Cell* **10:** 1107–1117

Milne TA, Dou Y, Martin ME, Brock HW, Roeder RG, Hess JL (2005) MLL associates specifically with a subset of transcriptionally active target genes. *Proc Natl Acad Sci USA* **102:** 14765–14770

Morillon A, Karabetsou N, Nair A, Mellor J (2005) Dynamic lysine methylation on histone H3 defines the regulatory phase of gene transcription. *Mol Cell* **18:** 723–734

Morris SA, Shibata Y, Noma K, Tsukamoto Y, Warren E, Temple B, Grewal SI, Strahl BD (2005) Histone H3 K36 methylation is associated with transcription elongation in *Schizosaccharomyces pombe*. *Eukaryot Cell* **4:** 1446–1454

Nakamura T, Mori T, Tada S, Krajewski W, Rozovskaia T, Wassell R, Dubois G, Mazo A, Croce CM, Canaani E (2002) ALL-1 is a histone methyltransferase that assembles a supercomplex of proteins involved in transcriptional regulation. *Mol Cell* **10:** 1119–1128

Nelson CJ, Santos-Rosa H, Kouzarides T (2006) Proline isomerization of histone H3 regulates lysine methylation and gene expression. *Cell* **126:** 905–916

Ng HH, Robert F, Young RA, Struhl K (2003) Targeted recruitment of Set1 histone methylase by elongating Pol II provides a localized mark and memory of recent transcriptional activity. *Mol Cell* **11:** 709–719

Pokholok DK, Harbison CT, Levine S, Cole M, Hannett NM, Lee TI, Bell GW, Walker K, Rolfe PA, Herbolsheimer E, Zeitlinger J, Lewitter F, Gifford DK, Young RA (2005) Genome-wide map of nucleosome acetylation and methylation in yeast. *Cell* **122:** 517–527

Rao B, Shibata Y, Strahl BD, Lieb JD (2005) Dimethylation of histone H3 at lysine 36 demarcates regulatory and nonregulatory chromatin genome-wide. *Mol Cell Biol* **25:** 9447–9459

Rayasam GV, Wendling O, Angrand PO, Mark M, Niederreither K, Song L, Lerouge T, Hager GL, Chambon P, Losson R (2003) NSD1 is essential for early post-implantation development and has a catalytically active SET domain. *EMBO J* **22:** 3153–3163

Ruthenburg AJ, Allis CD, Wysocka J (2007) Methylation of lysine 4 on histone H3: intricacy of writing and reading a single epigenetic mark. *Mol Cell* **25:** 15–30

Schaft D, Roguev A, Kotovic KM, Shevchenko A, Sarov M, Neugebauer KM, Stewart AF (2003) The histone 3 lysine 36 methyltransferase, SET2, is involved in transcriptional elongation. *Nucleic Acids Res* **31:** 2475–2482

Schneider R, Bannister AJ, Myers FA, Thorne AW, Crane-Robinson C, Kouzarides T (2004) Histone H3 lysine 4 methylation patterns in higher eukaryotic genes. *Nat Cell Biol* **6:** 73–77

Schübeler D, MacAlpine DM, Scalzo D, Wirbelauer C, Kooperberg C, van Leeuwen F, Gottschling DE, O'Neill LP, Turner BM, Delrow J, Bell SP, Groudine M (2004) The histone modification pattern of active genes revealed through genome-wide chromatin analysis of a higher eukaryote. *Genes Dev* **18:** 1263–1271

Shilatifard A (2006) Chromatin modifications by methylation and ubiquitination: implications in the regulation of gene expression. *Annu Rev Biochem* **75:** 243–269

Sims III RJ, Belotserkovskaya R, Reinberg D (2004) Elongation by RNA polymerase II: the short and long of it. *Genes Dev* **18:** 2437–2468

Strahl BD, Grant PA, Briggs SD, Sun ZW, Bone JR, Caldwell JA, Mollah S, Cook RG, Shabanowitz J, Hunt DF, Allis CD (2002) Set2 is a nucleosomal histone H3-selective methyltransferase that mediates transcriptional repression. *Mol Cell Biol* **22:** 1298–1306

Sun XJ, Wei J, Wu XY, Hu M, Wang L, Wang HH, Zhang QH, Chen SJ, Huang QH, Chen Z (2005) Identification and characterization of a novel human histone H3 lysine 36-specific methyltransferase. *J Biol Chem* **280:** 35261–35271

Thomson S, Clayton AL, Mahadevan LC (2001) Independent dynamic regulation of histone phosphorylation and acetylation during immediate-early gene induction. *Mol Cell* **8:** 1231–1241

Thomson S, Hollis A, Hazzalin CA, Mahadevan LC (2004) Distinct stimulus-specific histone modifications at hsp70 chromatin targeted by the transcription factor heat shock factor-1. *Mol Cell* **15:** 585–594

Thomson S, Mahadevan LC, Clayton AL (1999) MAP kinase-mediated signalling to nucleosomes and immediate-early gene induction. *Semin Cell Dev Biol* **10:** 205–214

Vakoc CR, Sachdeva MM, Wang H, Blobel GA (2006) Profile of histone lysine methylation across transcribed mammalian chromatin. *Mol Cell Biol* **26:** 9185–9195

Xiao T, Hall H, Kizer KO, Shibata Y, Hall MC, Borchers CH, Strahl BD (2003) Phosphorylation of RNA polymerase II CTD regulates H3 methylation in yeast. *Genes Dev* **17:** 654–663

Zhou M, Deng L, Lacoste V, Park HU, Pumfery A, Kashanchi F, Brady JN, Kumar A (2004) Coordination of transcription factor phosphorylation and histone methylation by the P-TEFb kinase during human immunodeficiency virus type 1 transcription. *J Virol* **78:** 13522–13533

